Thin Solid Films 519 (2010) 818–822

Contents lists available at ScienceDirect

Thin Solid Films

journal homepage: www.elsevier.com/locate/tsf

Forming wrinkled stiff films on polymeric substrates at room temperature for stretchable interconnects applications

Cunjiang Yu, Hanqing Jiang *

School of Mechanical, Aerospace, Chemical and Materials Engineering, Arizona State University, Tempe, AZ 85287, United States

ARTICLE INFO

Article history:
Received 4 April 2010
Received in revised form 6 August 2010
Accepted 17 August 2010
Available online 25 August 2010

Keywords:
Stretchable electronics
Wrinkle
Polydimethylsiloxane
Thins films

ABSTRACT

Periodically wrinkled stiff thin films on elastomeric substrates have been found extensive applications, such as in stretchable electronics. This paper presents a cost-effective and simple method to form wrinkled stiff SiO_x thin films on polydimethylsiloxane (PDMS) substrates at room temperature by ultraviolet/ozone (UV/O) radiation on pre-strained PDMS. Systemic studies have been conducted to understand the dependence of the wavy profile on the PDMS pre-strain, UV/O exposure time, and PDMS modulus. The mechanics analysis has been verified to be quantitatively or qualitatively accurate by experimental comparisons. The wrinkled SiO_x/PDMS system is stretchable and provides a wavy mold for stretchable electrodes. The constant electrical resistance during mechanical stretching shows the stretchability of this system.

© 2010 Elsevier B.V. All rights reserved.

1. Introduction

Stretchable electronics, an emerging area of electronics, has been attracting extensive attentions and opened the door to many potential applications, such as transistors [1,2], circuits [3], sensors [4], electronic eyes [5], energy components [6], which current rigid electronics cannot realize. The mechanical instability of stiff thin films (e.g., single crystalline Si) on compliant substrate (e.g., polydimethylsiloxane (PDMS)), which was used to achieve the stretchability of brittle materials, has been experimentally and theoretically studied [7–10]. The method used to obtain this buckling is to transfer [1–6] or deposit [11–15] stiff thin films onto a pre-strained PDMS substrate followed by the relaxation of the pre-strained substrate, which leads to buckled patterns in the stiff thin films with well defined wavelength and amplitude. On one hand, the interfacial bonding between the stiff thin films and elastomeric substrate has to be sufficiently strong to transfer the load to trigger the buckling; therefore, multi-steps are involved, especially for the transfer method, to ensure the strong bonding. On the other hand, a more cost-effective, technologically simple process without using conventional lithography, as one of the most significant driving forces for developing macroelectronics, is highly desired. Other than deposit or transfer thin stiff films on PDMS to realize buckling, this article focuses on an alternative method in which the metal film is conformal to a compliant sinusoidally contoured substrate. The contoured substrate comprises a wavy stiff thin SiO_x film on a PDMS substrate, formed by ultraviolet/ozone (UV/O) treatment on pre-stretched PDMS substrate followed relaxation. The metal thin film/contoured substrate is stretchable and has been demonstrated as stretchable electrical conductors.

2. Experiment

PDMS was prepared by mixing silicone elastomer base and curing agent (Sylgard 184, Dow Corning) at the ratio of 10:1 by weight, followed by degas and polymerization at 80 °C for 2 h. The polymerized PDMS slab (1 mm thick, 1 cm wide, and 2 cm long) is stretched by a stage to desired pre-strain ε_{pre}, as shown in step (i) in Fig. 1. The pre-strained PDMS substrate is subject to a flood exposure by a UV lamp (low pressure mercury lamp, BHK), which generates 185 nm and 254 nm radiations to react and change the chemistries of PDMS at the presence of atmosphere oxygen, as shown in step (ii) in Fig. 1. The distance between the lamp and the sample is constant 5 mm, which is chosen in order to maintain high radiation intensity 0.51 mW/cm^2, but not to introduce much perturbation by the heat from the lamp. The exposing time varies from 40 min to 140 min, and the pre-strain on PDMS varies from 10% to 40%. The PDMS exhibits creep behavior after subjected to a fixed deformation for a significant amount of time, and it becomes more dramatic when PDMS is heated up. For example, there is around 5% permanent strain on PDMS after a 20% pre-strain is held for 120 min during UV/O treatment. Once the desired exposure time is reached, the pre-strained PDMS is slowly relaxed to generate wavy surfaces, as illustrated by step (iii) of Fig. 1. The fabricated wavy PDMS sample surface is characterized by optical microscopy and scanning electron microscopy (SEM). A 3 nm-thick gold/palladium layer is sputtered for discharging purpose prior to

* Corresponding author. Tel.: +1 480 965 1483.
E-mail address: Hanqing.jiang@asu.edu (H. Jiang).

0040-6090/$ – see front matter © 2010 Elsevier B.V. All rights reserved.
doi:10.1016/j.tsf.2010.08.106

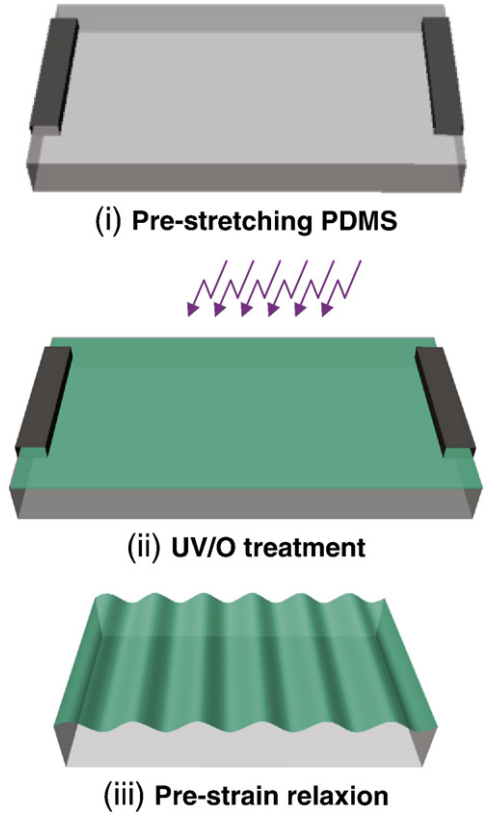

Fig. 1. Schematic illustration of the fabrication process.

SEM imaging. The amplitude and wavelength are characterized by profilometer. To demonstrate the application for stretchable electrodes, chromium/gold (Cr/Au) films are directly deposited on the sinusoidally contoured surface by thermal evaporation through a shadow mask. Cr serves as adhesive promoter between SiO_x and gold. The electrical resistances of the electrodes are characterized using Hewlett–Packard (HP) 4061-A semiconductor testing system. The modulus of the softer PDMS (mixing ratio of base and curing agent is 20:1) is derived from the tensile experiment of PDMS slabs based on a custom made tensile testing setup.

3. Results and discussion

Different from usual processes to fabricate silicon oxide films by employing high temperature or requiring high vacuum environment to convert siloxane to silicon oxide compound [16,17], UV/O reaction with cross-linked PDMS offers an alternative approach at room temperature and without any strict environmental requirement [18,19]. The 185 nm radiations from the lamp produce ozone, while the 254 nm radiations dissociate the ozone to O_2 and atomic oxygen (O). The later species are the chief reactant to react with PDMS [18,19]. The reaction proceeds based on the diffusion of ozone to meet PDMS; therefore, the oxidization initiates at the PDMS surface and gradually penetrates into the PDMS. Upon oxidization, the organic portion of PDMS, presenting as carbon dioxide, water, and some amount of volatile organic compounds, escapes from the PDMS substrate; while the silicon components do not form volatile compounds and thus, a residual thin film of SiO_x is formed [19]. More explicitly, the UV/O treatment on a pre-strained PDMS eventually generates a thin SiO_x film on a pre-strained PDMS substrate, which is comparable to the method using oxygen plasma treatment over PDMS [20].

Releasing the pre-strain on the PDMS, thin SiO_x film supported by PDMS substrates spontaneously buckles, which has been reported elsewhere [21,22]. However, hierarchy wrinkling patterns with wrinkling wavelength at submicron scale as reported by Ref. [21] was not observed despite that similar methods were used. The physical mechanism for buckling is that the stiff thin film tends to buckle to release the compressive strain imposed by the relaxation of the pre-stretched substrate. From the energy point of view, the total energy in the thin film/substrate system is released by introducing the bending energy due to the out-of-plane deformation (buckle) of the thin films. Mechanics models have been developed to understand these systems based on energy method [7–10]. The buckling period and amplitude can be characterized by [9],

$$\lambda = \frac{2\pi h_f}{\left(1+\varepsilon_{pre}\right)(1+\xi)^{\frac{1}{3}}}\left[\frac{E_f\left(1-\nu_s^2\right)}{3E_s\left(1-\nu_f^2\right)}\right]^{\frac{1}{3}}, \tag{1}$$

$$A = \frac{h_f}{\sqrt{1+\varepsilon_{pre}(1+\xi)^{\frac{1}{3}}}}\sqrt{\frac{\varepsilon_{pre}}{\varepsilon_c}-1}, \tag{2}$$

where $\xi = \frac{5}{32}\varepsilon_{pre}\left(1+\varepsilon_{pre}\right)$ represents the large deformation and geometrical nonlinearity in the substrate and $\varepsilon_c = \frac{1}{4}\left[\frac{3E_s\left(1-\nu_f^2\right)}{E_f\left(1-\nu_s^2\right)}\right]^{\frac{2}{3}}$ denotes the critical buckling strain or the minimum strain needed to achieve buckling. E is the Young's modulus; ν is the Poisson's ratio, and the subscripts s and f refer to the substrate and stiff thin film, respectively. h_f is the thickness of the stiff thin film. Fig. 2 shows the

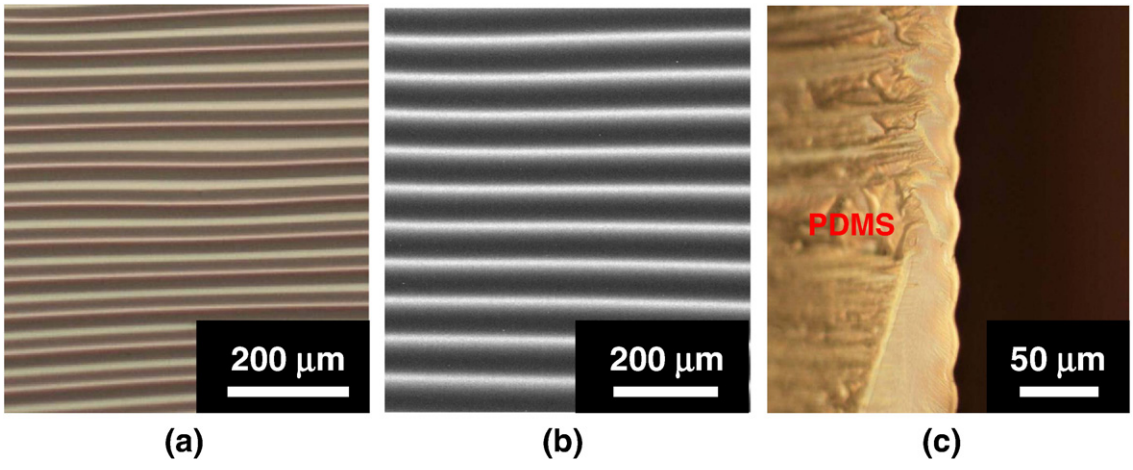

Fig. 2. (a) and (b): Optical and SEM image of the wrinkled SiO_x/PDMS, respectively; (c) optical image of the cross section of the periodic wrinkling profile.

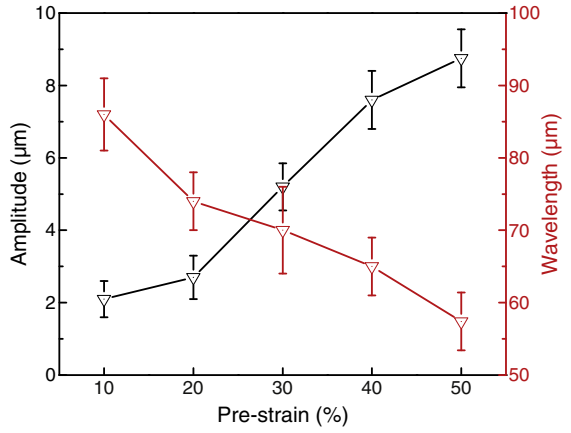

Fig. 3. For unchanged exposure time of 80 min, the amplitude increases, while the wavelength decreases, as increasing the pre-strain.

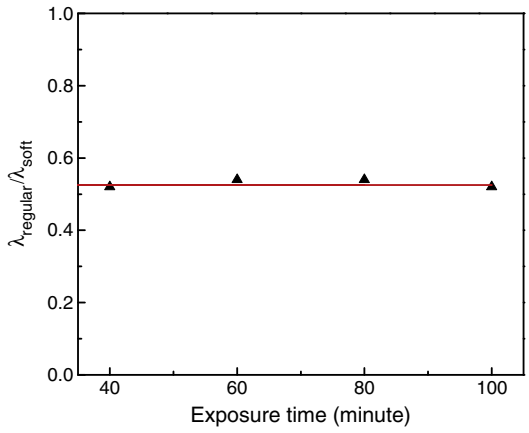

Fig. 5. The ratio of the wavelength for buckled stiff thin SiO_x films on regular PDMS (10:1 base and curing agent mixing ratio) and soft PDMS (20:1 mixing ratio) remains constant with various exposure time.

optical (a and c) and SEM image (b) of the sinusoidal wrinkling samples fabricated by exposing UV/O for 80 min on a PDMS substrate subject to 20% pre-strain. The cracks are generated due to the Poisson's effect during the relaxation of the pre-strain. The SiO_x layer is subjected to compressive strain in the pre-strain direction and tensile strain in the width direction. The compressive strain leads to buckling and the latter results in cracks along the width direction. The density of crack is very low so that the cracks are not shown in Fig. 2a with about 800 μm × 600 μm view.

The dependence of the buckling profiles (amplitude and wavelength) on the pre-strain level and the exposure time of UV/O have been systematically studied. To create moderate wrinkling patterns with tens of micron period, exposure time longer than 40 min and pre-strain greater than 10% are investigated in this study. For shorter exposure time and smaller pre-strain, no obvious wrinkling patterns has been observed.

The case with various pre-strain levels and fixed UV/O exposure time has been studied. For fixed UV/O exposure time, it is reasonable to assume that the extent of oxidization is unchanged and thus the formed SiO_x thin film keeps the same. In other words, h_f and E_f in Eqs. (1) and (2) are constants, and only the pre-strain ε_{pre} varies. As indicated by Eqs. (1) and (2), amplitude increases and wavelength decreases with the increase of the pre-strain, also as confirmed by Fig. 3, in which the buckling amplitude (left axis, black) and wavelength (right axis, red) of the wavy profile vary with pre-strain for constant exposure time of 80 min.

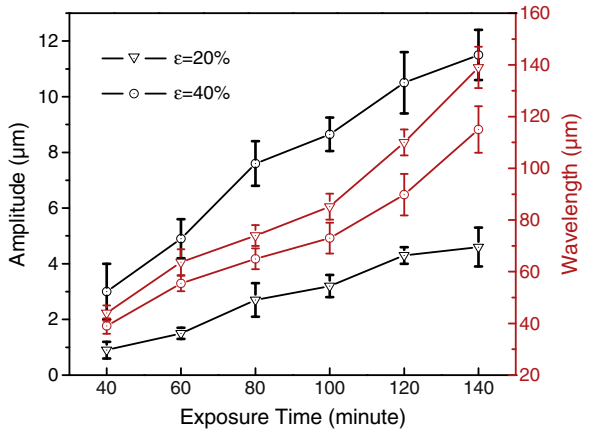

Fig. 4. The amplitude and wavelength of the wrinkling profile increase when the exposure time increases.

Fig. 3 also provides a means to estimate the thickness of the SiO_x thin film for known PDMS properties ($E_s = 2$ MPa, $\nu_s = 0.49$) [23] and pre-strain ε_{pre} if E_f is taken as the modulus of SiO_2 ($E_f = 75$ GPa, $\nu_f = 0.3$). By using the method of least square, the thickness of SiO_x thin film is estimated as 289 nm, which is much higher than the values reported on the order of tens of nanometers [18,24]. We believe that abundant atmospheric oxygen from the open environment in our experiments should be responsible for thicker stiff film. It is noted that this method can only provide an estimation of the thickness of the SiO_x thin film since the properties of the thin film may have gradient from the top to the bottom as the intensity of the UV/O irradiation gradually decays. In other words, the thin film is a non-uniform material but relatively stiffer at the top and softer at the bottom.

Different from the abovementioned case, experiment with various UV/O exposure time and fixed pre-strain has also been explored. It is intuitive that the film becomes thicker as the exposure time increases. When h_f increases, as indicated by Eqs. (1) and (2), both the amplitude A and wavelength λ increase. This trend is also shown in Fig. 4, in which the exposing time increases from 40 to 140 min, the measured wavelength increase from 44 to 155 μm, and the amplitude increases from 0.45 to 4.6 μm for 20% pre-strain; and the wavelength increases from 39 to 115 μm, and the amplitude increases from 3 to 11.5 μm for 40% pre-strain.

The previous two cases, independently changing exposure time and pre-strain, have shown that the buckling analysis given by Eqs. (1) and (2) can capture the trend shown in Figs. 3 and 4. The effect the PDMS modulus has further been studied. As indicated by Eq. (1), the wavelength depends on the modulus ratio of thin film and substrate. By fixing the exposure time or equivalently constant thin film thickness and modulus, and levels of pre-strain, changing the modulus of PDMS can further examine the buckling analysis given by Eq. (1). The modulus of PDMS can be tuned by varying the mixing ratio of the base polymer and curing agent. For example, the modulus of PDMS with a 20:1 mixing ratio of base polymer and curing agent is about 0.29 MPa, which is about one order different from 2.0 MPa of the regular PDMS with 10:1 mixing ratio. Fig. 5 shows the ratio of buckling wavelength of stiff thin SiO_x film on regular PDMS (10:1) and soft PDMS (20:1) versus the exposure time. The experimental data (marked as solid upper triangles) agree very well with the red line that corresponds to the theoretical solution, i.e., $\lambda_{regular}/\lambda_{soft} = (E_s^{soft}/E_s^{regular})^{1/3} = 0.525$. Therefore, this experiment further verifies that the buckling analysis Eqs. (1) and (2) capture the physics of the buckled stiff thin films on compliant substrates.

The wrinkled SiO_x/PDMS produced by relaxing the pre-strain after UV/O exposure is reversibly stretchable. To study its stretchability, thin metal conductors of 5/50 nm-thick chromium/gold (Cr/Au) are

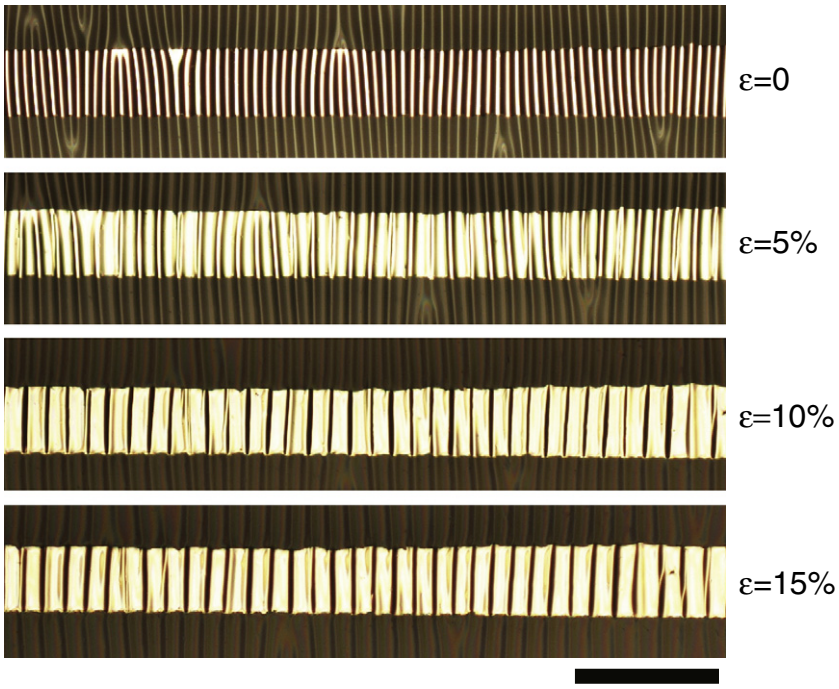

Fig. 6. Optical images of the stretchable electrodes under different levels of applied strain. The scale bar is 500 μm.

deposited by thermal evaporation through a shadow mask on the wavy SiO_x/PDMS surface as the stretchable electrode, followed by the electrical resistance measurement. Fig. 6 shows the optical images of the stretchable electrodes, 2 cm long and 250 μm wide, at different applied strain levels, i.e., the strains post applied on the buckled SiO_x/PDMS. The pre-strain on the wavy SiO_x/PDMS is 17.5% and the UV/O exposure time is 60 min. The compressive strain on the wavy stiff thin film is 12.5% due to the creep behavior of the PDMS. The buckling wavelength increases as the sample are stretched, similar to the accordion bellows. The electrical resistance shown in Fig. 7 initially maintains unchanged at small (below 12.5%) applied strain in the pre-stretch direction, followed by sharp increase caused by the appearance of cracks upon further stretching. The creep behavior of the PDMS attributes to the difference in the pre-strain (17.5%) and the applied strain (12.5%) at which the resistance increases significantly.

We note that there are cracks in the perpendicular direction to the applied strain (Fig. 8), which is different from the cracks of SiO_x layer that is along the pre-strain direction. The cracks mainly appear at the peak or valley of the Cr/Au film, which suggests that these cracks are led by the applied strain in tension. To avoid the extreme condition in which the applied strain approaches the pre-strain, one can mechanically stretch such conductor at moderate strain level but to remain electrical conducting.

Thus, the wavy SiO_x/PDMS surface provides an easy way for stretchable electrode applications, which is different from previously reported methods, such as directly coating metal films on tensioned [15] or untensioned PDMS [25,26] or on wavy PDMS surface resulting from relief molding of fabricated wavy structures by micromachining technology [27], and helix spring-like microwires [28]. These methods either can only deposit very thin metals (e.g., 25 nm-thick gold in Ref. [25]), which are not desired for conductor applications, or involve multi-step fabrications (e.g., anisotropic silicon etching, mold surface smoothening, PDMS casting and peeling-off in Ref. [27]). Moreover, this surface also provides a wavy mold for three-dimensional forming, such laser dynamic forming [29] for potential high-throughput

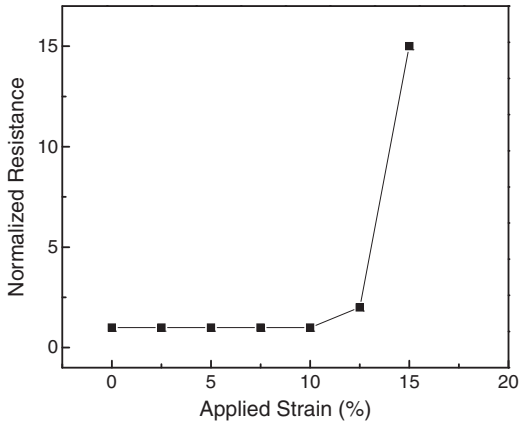

Fig. 7. The normalized resistance of the electrode verses the applied strain. The original resistance is 165 Ω.

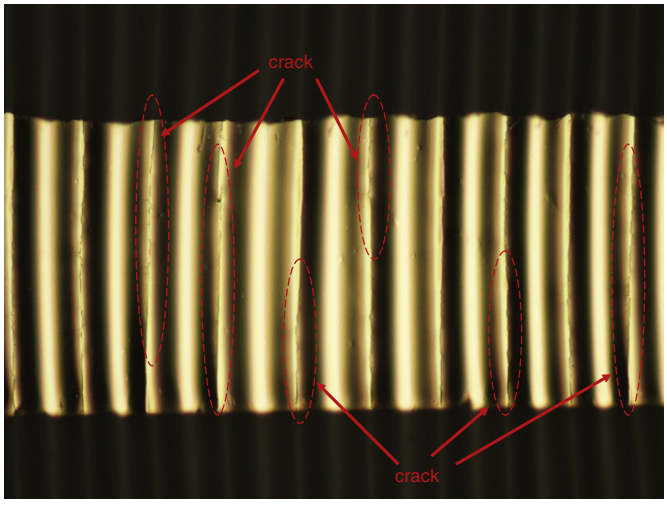

Fig. 8. The cracks in the conductor appear perpendicular to the stretching direction after large level (17.5%) of stretching. The scale bar is 100 μm.

manufacturing. The cracking due to the Poisson's effect after the relaxation of the pre-strain is the main disadvantage of this method, which can be resolved by an alternative stretching stage. Specifically, a stage with prescribed stretching in one direction and a constraint displacement on the perpendicular direction can eliminate the Poisson's effect.

4. Conclusions

This paper has shown a cost-effective and simple method to fabricate wrinkling structures. SiO_x stiff film has been produced at room temperature by radiating UV/O on PDMS. Systemic studies have been conducted to understand the dependence of the wavy profile on the PDMS pre-strain, UV/O exposure time, and PDMS modulus. The mechanics analysis has been verified to be quantitatively or qualitatively accurate by experimental comparisons. The wrinkled SiO_x/PDMS system is stretchable and its stretchability has been studied by measuring the electrical resistance that keeps unchanged for moderate strain levels. The wavy SiO_x/PDMS surface provides an alternative and easy way for stretchable electrode applications. For future integration as a stretchable system, more investigations such as either to directly fabricate other electrical components such as transistors with the electrodes or to transfer thin film based elements to elastomer substrates with stretchable electrodes for full integration.

Acknowledgements

HJ acknowledges the support from NSF CMMI-0700440.

References

[1] D.Y. Khang, H. Jiang, Y. Huang, J.A. Rogers, Science 311 (2006) 208.
[2] Y. Sun, W.M. Choi, H. Jiang, Y.Y. Huang, J.A. Rogers, Nat. Nanotechnol. 1 (2006) 201.
[3] D.H. Kim, J.H. Ahn, W.M. Choi, H.S. Kim, T.H. Kim, J. Song, Y.Y. Huang, z. Liu, C. Lu, J. A. Rogers, Science 320 (2008) 507.
[4] C. Yu, Z. Wang, H. Yu, H. Jiang, Appl. Phys. Lett. 95 (2009) 141912.
[5] H.C. Ko, M.P. Stoykovich, J. Song, V. Malyarchuk, W.M. Choi, C.-J. Yu, J.B. Geddes, J. Xiao, S. Wang, Y. Huang, J.A. Rogers, Nature 454 (2008) 748.
[6] C. Yu, C. Masarapu, J. Rong, B. Wei, H. Jiang, Adv. Mater. 21 (2009) 4793.
[7] R. Huang, J. Mech. Phys. Solids 53 (2005) 63.
[8] Z. Huang, W. Hong, Z. Suo, J. Mech. Phys. Solids 53 (2005) 2101.
[9] H. Jiang, D.Y. Khang, J. Song, Y. Sun, Y. Huang, J.A. Rogers, Proc. Natl Acad. Sci. USA 104 (2007) 15607.
[10] H. Jiang, D.Y. Khang, H. Fei, H. Kim, Y. Huang, J. Xiao, J.A. Rogers, J. Mech. Phys. Solids 56 (2008) 2585.
[11] N. Bowden, S. Brittain, A.G. Evans, J.W. Hutchinson, G.M. Whitesides, Nature 393 (1998) 146.
[12] S.P. Lacour, S. Wagner, Z. Huang, Z. Suo, Appl. Phys. Lett. 82 (2003) 2404.
[13] S.P. Lacour, J. Jones, S. Wagner, T. Li, Z. Suo, Proc. IEEE 93 (2005) 1459.
[14] C. Yu, K. O'Brien, Y.-H. Zhang, H. Yu, H. Jiang, Appl. Phys. Lett. 96 (2010) 041111.
[15] S. Lacour, J. Jones, Z. Suo, S. Wagner, IEEE Electron Device Lett. 25 (2004) 179.
[16] M. Nyman, S. Desu, C. Peng, Chem. Mater. 5 (1993) 1636.
[17] T. Maruyama, T. Tago, Thin Solid Films 232 (1993) 201.
[18] M. Ouyang, C. Yuan, R.J. Muisener, A. Boulares, J.T. Koberstein, Chem. Mater. 12 (2000) 1591.
[19] M. Ouyang, R.J. Muisener, A. Boulares, J.T. Koberstein, J. Membr. Sci. 177 (2000) 177.
[20] N. Bowden, W.T. Huck, K.E. Paul, G.M. Whitesides, Appl. Phys. Lett. 75 (1999) 2557.
[21] K. Efimenko, M. Rackaitis, E. Manias, A. Vaziri, L. Mahadevan, J. Genzer, Nat. Mater. 4 (2005) 293.
[22] J. Genzer, J. Groenwold, Soft Matter 2 (2006) 310.
[23] A. Bietsch, B. Michel, J. Appl. Phys. 88 (2000) 4310.
[24] K. Efimenko, W.E. Wallace, J. Genzer, J. Colloid Interface Sci. 254 (2002) 306.
[25] S.P. Lacour, D. Chan, S. Wagner, T. Li, Z. Suo, Appl. Phys. Lett. 88 (2006) 204103.
[26] N. Lu, X. Wang, Z. Suo, J. Vlassak, Appl. Phys. Lett. 91 (2007) 221909.
[27] J. Xiao, A. Carlson, Z.J. Liu, Y. Huang, H. Jiang, J.A. Rogers, Appl. Phys. Lett. 93 (2008) 013109.
[28] S. Befahy, S. Yunus, T. Pardoen, P. Bertrand, Appl. Phys. Lett. 91 (2007) 141911.
[29] C. Yu, H. Gao, H. Yu, H. Jiang, G.J. Cheng, Appl. Phys. Lett. 95 (2009) 091108.